Dalton Transactions

Accepted Manuscript

ROYAL SOCIETY OF CHEMISTRY

www.rsc.org/dalton

Tunable optical properties for hybrid inorganic-organic $[(TiO_2)_m(Ti\text{-}O\text{-}C_6H_4\text{-}O\text{-})_k]_n$ superlattice thin films

*Janne-Petteri Niemelä, Maarit Karppinen**

Department of Chemistry, Aalto University, FI-00076 Aalto, Finland

A combined atomic layer deposition (ALD) and molecular layer deposition (MLD) process was developed to fabricate inorganic-organic $[(TiO_2)_m(Ti\text{-}O\text{-}C_6H_4\text{-}O\text{-})_k]_n$ thin films from $TiCl_4$, water and hydroquinone (HQ) precursors, and in particular, superlattice structures where single-molecular organic layers (k=1) are periodically sandwiched between thicker TiO_2 layers (m>1). The incorporation of organic layers was found to systematically blue-shift the optical band gap of TiO_2 with decreasing superlattice period, and – most importantly – to sensitize the TiO_2 layers to visible light over a considerable part of the visible range below 700 nm, a fact that could be of substantial interest in photocatalysis and solar cell applications.

Corresponding Author**:**

*Email: maarit.karppinen@aalto.fi

Introduction

The conventional strategies for enhancing optical and electrical properties of inorganic materials are typically based on small modifications in composition through e.g. extrinsic cation substitutions or oxygen-content control. An attractive alternative approach to tune the materials' properties is offered by assembly of inorganic-organic hybrid structures where not only can the organic component be used to enhance the performance of the inorganic matrix, but also completely new material properties can be expected as the distinct natures of the organic and inorganic components are combined in a single material.[1-3]

Among the hybrid materials, inorganic-organic superlattices constitute a particularly interesting material family, as the compositional synergies provided by the hybrid framework are combined with the freedom to tune the dimensions of the inorganic and organic material domains in nanoscale by controlling the superlattice period.[4,5] Thereby, enhanced control over the material properties, including quantum effects, is enabled in hybrid superlattices. Synthesis of such regular two-dimensional thin-film structures requires a very precise atomic-level control over the chemistries that determine the inorganic-organic interface structures upon film growth. The deposition processes should hence be based on self-saturating surface reactions. Moreover, the deposition processes for the inorganic and organic component materials must be chemically compatible and feasible simultaneously in a single deposition chamber. Employing molecular layer deposition (MLD) in combination with atomic layer deposition (ALD) provides an ideal set of techniques to meet these criteria for inorganic-organic superlattice thin-film fabrication.

The ALD technique is a chemical vapor deposition variant that relies on the condition of self-terminating reactions on a substrate surface. Such condition is met by transporting the precursor

vapors to the substrate one after another and purging the reactor chamber after each precursor pulse with flowing inert gas. A sequence consisting of at least two precursor pulses and subsequent purging for each precursor is called an ALD cycle. Ideally one ALD cycle deposits an atomic monolayer of the target compound, and thus the film thickness is accurately controlled by the total number of cycles. Thanks to the self-terminating surface reactions ALD provides an enabling technique to uniformly and conformally deposit thin films on large-area substrates and high-aspect-ratio three-dimensional nanostructures. Currently, synthesis of a wide variety of compounds ranging from binary oxides, nitrides and sulfides to more complex ternary and doped thin films can be realized with ALD.[6-9]

Molecular layer deposition is a thin-film fabrication technique analogous to ALD but based on purely organic precursors. Accordingly, in MLD deposition of molecular monolayers instead of atomic monolayers is allowed for.[10,11] Molecular layer deposition can be used to fabricate thin films of organic polymers, such as polyamides and polyimides.[12,13] Most interestingly, use of metal precursors together with organic precursors enables hybrid inorganic-organic thin films to be fabricated with combined ALD/MLD processes,[14,15] where the organic precursors can be, *e.g.*, organic alcohols[14,16] or carboxylic acids.[17,18] Such combined ALD/MLD processes also allow for fabrication of hybrid inorganic-organic materials in the form of nanolaminates[19-21] and superlattices[22-24] in an elegant manner.

Titanium dioxide is an inorganic semiconductor well known for its photocalytic properties[25] and widely used as a dye sensitized solar cell electrode material.[26] For such photoelectrochemical applications, the wide 3.2 eV band gap of pure TiO_2 limits the full exploitation of the solar spectrum, and hence, sensitization of TiO_2 to visible light plays a key role in search for enhanced

device performance. In this respect, combining ALD fabricated TiO_2 layers with MLD fabricated organic layers into hybrid structures provides an attractive way for tuning the optical properties of TiO_2. A good candidate for an MLD precursor to fabricate the hybrid films for this purpose is hydroquinone (HQ), as it is rich in π-electrons that could potentially be active in interaction with the inorganic layers, and moreover, it provides controllable growth with its rigid aromatic backbone hindering unwanted double reactions with the surface during the film deposition.[15]

In this work, we report the successful fabrication of inorganic-organic $[(TiO_2)_m(Ti\text{-}O\text{-}C_6H_4\text{-}O\text{-})_{k=1}]_n$ superlattice thin films deposited with an ALD/MLD technique in a wide range of compositions. In order to fabricate the superlattice films, an ALD/MLD process for hybrid $(Ti\text{-}O\text{-}C_6H_4\text{-}O\text{-})_k$ thin films from $TiCl_4$ and hydroquinone precursors was at first developed. X-ray reflectivity and infrared spectroscopy were employed to verify the intended superlattice structures, whereas UV-Vis spectroscopy provided the means for observing a gradual blue-shift of the band gap in the TiO_2 layers with decreasing superlattice period and for verification of a sensitization of the TiO_2 layers to visible light with the organic layers.

Results and discussion

Our ALD/MLD process from $TiCl_4$ and HQ precursors, illustrated in Fig. 1(a), yielded smooth and partially transparent hybrid $(Ti\text{-}O\text{-}C_6H_4\text{-}O\text{-})_k$ films of orange/red color in appearance. In order to find the conditions required for self-limiting film growth, the precursor pulse lengths were varied between 0.5-20 s for HQ and between 0.1-0.4 s for $TiCl_4$ (Fig. 2). The resultant films were analyzed for the thickness using the XRR data. The GPC values were calculated dividing the film thicknesses by the total number of deposition cycles. Based on the film thickness vs. pulse length data, for HQ exposure the surface reaction was found to reach completion after

around 10 s whereas for $TiCl_4$ exposure the surface reaction saturated for all the pulse lengths studied. Thereby, 15 s pulse length with 30 s purge for HQ and 0.2 s pulse length with 4 s purge were fixed for the following depositions. Hybrid films with various thicknesses were then deposited corresponding to total cycle numbers of 100, 200 and 500. The film growth exhibited linear behavior as a function of cycle number and a growth per cycle (GPC) value of 3.1 Å/cycle was determined from the slope of the linear fit to the film thickness vs. cycle number data. In the ideal picture based on the expected bond lengths of vertically aligned Ti-O-C_6H_4-O- chains growth of around 10 Å/cycle could be reached. Hence, the present ALD/MLD process probably suffered from some non-idealities such as molecule tilting or double reactions of hydroquinone –OH groups with the –Cl groups of the surface. The GPC value is however in line with the reported values for Ti-based ALD/MLD films with other organic precursors: for films from $TiCl_4$ and glycerol growth per cycle values ranged between 2.1 Å/cycle (210 ^{o}C) and 2.8 Å/cycle (130 ^{o}C), whereas for films from $TiCl_4$ and ethylene glycol the growth was 4.5 Å/cycle (95-115 ^{o}C) and 1.5 Å/cycle (135 ^{o}C).[27]

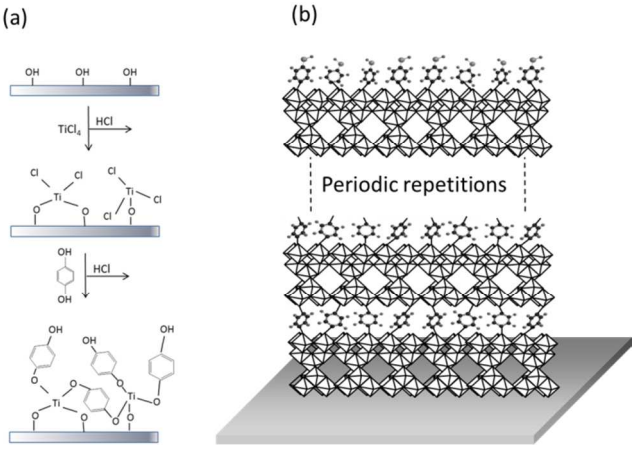

Figure 1. A schematic representation of the deposition process for one cycle (k=1) of (Ti-O-C_6H_4-O-)$_k$ hybrid (a). A schematic representation of the superlattice film structure where single cycles of (Ti-O-C_6H_4-O-)$_{k=1}$ hybrid are deposited, as illustrated in image (a), between octahedrally coordinated TiO_2 layers to form [$(TiO_2)_m$(Ti-O-C_6H_4-O-)$_{k=1}$]$_n$ superlattices (b).

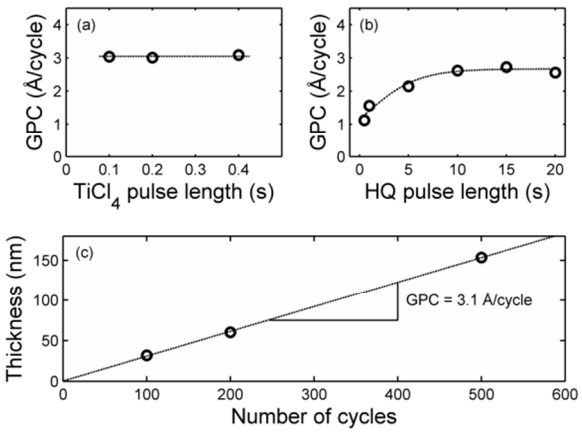

Figure 2. Deposition characteristics as determined by X-ray reflectivity for hybrid inorganic-organic (Ti-O-C_6H_4-O-)$_k$ thin films from $TiCl_4$ and hydroquinone (HQ) precursors. Growth per cycle (GPC) values with varying pulse length for $TiCl_4$ (a) and for hydroquinone (HQ) (b). Thickness vs. number of $TiCl_4$/HQ cycles k (c).

The fabrication route developed for the hybrid (Ti-O-C_6H_4-O-)$_k$ films was then combined with the $TiCl_4/H_2O$ ALD process for TiO_2 in order to grow [$(TiO_2)_m$(Ti-O-C_6H_4-O-)$_{k=1}$]$_n$ superlattice structures with single molecular organic layers sandwiched between wider inorganic layer blocks (Fig. 1(b)). The growth of the superlattice films depended systematically on the film composition as is shown in Fig. 3. The GPC values were found to increase from around 0.40 Å/cycle to 0.68 Å/cycle as the k:m ratio increased from 1:400 to 1:4. Such increasing trend was expected as with increasing k:m ratio more and more $TiCl_4$/HQ cycles with a high GPC value of 3.1 Å/cycle contribute to the overall GPC value. The systematic changes in the GPC values indicate that the

deposition process for the hybrid (Ti-O-C_6H_4-O-)$_k$ films was mixed in a controlled manner with the process for the TiO_2 films by the present ALD/MLD technique.

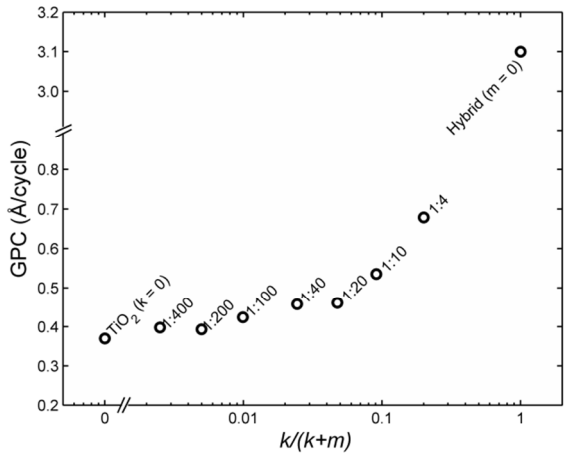

Figure 3. Growth per cycle values (GPC) for the [(TiO_2)$_m$(Ti-O-C_6H_4-O-)$_{k=1}$]$_n$ superlattice films as determined by X-ray reflectivity.

Crystallinity of the thin-film samples deposited on glass substrates was then studied with GIXRD (Fig. 4). The diffraction peaks of the purely inorganic ALD film were readily indexed to 101, 103, 004, 112, 200, 105 and 211 reflections of the anatase crystal structure of TiO_2. For the 1:400 sample the intensity of the peaks reduced notably, implying that the introduction of the organic molecules into the structure hindered the crystallization of TiO_2. For k:m > 1:400 no reflections were detected which indicated the formation of amorphous superlattices.

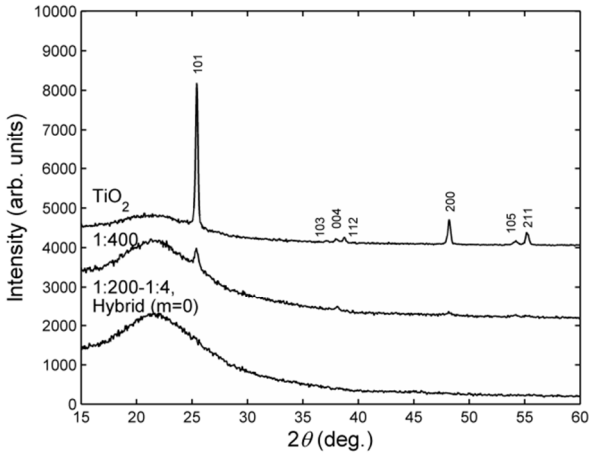

Figure 4. Grazing incidence X-ray diffraction patterns for the $[(TiO_2)_m(Ti\text{-}O\text{-}C_6H_4\text{-}O\text{-})_{k=1}]_n$ superlattice films.

The XRR technique was employed to verify the targeted superlattice structures as illustrated in Fig. 5 for the 1:400, 1:200 and 1:100 samples. From around θ = 0.1° until the critical angle around 0.25°, the reflected intensity experienced a plateau of maximum intensity corresponding to the total reflection of the primary beam. After the critical angle the intensity rapidly decreased followed by an onset of periodic oscillations of the reflected intensity. The small fringes correspond to the interference minima and maxima of reflected beam from the film-air and film-substrate interfaces and hence depend on the film thickness. In addition to the small fringes, the reflected intensity also showed periodically repeated interference maxima with higher intensity. These higher maxima stemmed from constructive interference from the periodically positioned organic layers. The angular difference of the maxima relates to the spatial separation of the successive organic layers, that is, the superlattice period. Hence obtained superlattice periods multiplied by the number of their repetitions corresponded well with the measured film thicknesses. The number of the small and large fringes relative to each other carries information on the total number of the superlattice period repetitions *n*. Ideally, *n*-2 gives the number of small

fringes found between the successive large fringes. For the 1:400 and 1:200 samples this was found to hold as *n* obtained from the reflection patterns matched the corresponding experimental deposition parameter. The angular separation of the reflection maxima is directly proportional to the number of repetitions of the superlattice period and hence, in the θ range with measurable intensities, superlattice structures for *k*:*m* ratios larger than 1:100 could not be detected. The observation of the higher intensity maxima in the XRR patterns proves that the organic molecules were periodically deposited between the TiO_2 layers and verifies that superlattice structures with precise interface control were synthesized in a predicted manner.

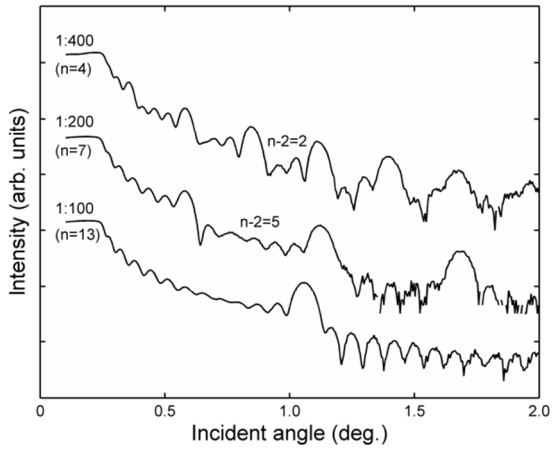

Figure 5. X-ray reflectivity patterns for the $[(TiO_2)_m(Ti\text{-}O\text{-}C_6H_4\text{-}O\text{-})_{k=1}]_n$ films with *k*:*m* ratios of 1:400, 1:200 and 1:100. Angular spacing of the small fringes relates to total film thickness, whereas that of the large ones carry information on the superlattice period *n*.

In order to study the chemical state of the films, they were measured for their absorbance of mid-infrared radiation in the wave number range of 400-4000 cm^{-1}. The transmittance spectra of the $[(TiO_2)_m(Ti\text{-}O\text{-}C_6H_4\text{-}O\text{-})_k]_n$ films at normal angle of incidence obtained via FTIR technique are presented in Fig. 6. The most pronounced feature in the FTIR spectra was the very clear absorption peak at around 1486 cm^{-1} corresponding to the C=C stretching in the aromatic rings

from the HQ precursor. Together with a weak aromatic ring signal at 1589 cm^{-1}, this implied that the aromatic rings were delivered to the film structure intact. The presence of a broad C-O stretching signal at around 1196 cm^{-1} indicated that the aromatic rings readily bonded via oxygen atoms to the TiO_2 matrix. The presence of the TiO_2 layers was witnessed as Ti-O absorption was found to peak between 400 and 500 cm^{-1} with increasing intensity for decreasing *k*:*m*. A weak signal at around 833 cm^{-1} corresponded to the C-H bend of *para*-substituted aromatic rings, whereas the presence of a small peak at 886 cm^{-1} could stem from 1,2,4-trisubstituted aromatic rings as an indication of some unexpected side reactions. Very small peaks were seen at 441 and 494 cm^{-1}, particularly for the *m*=0 hybrid, probably due to Ti-Cl bond absorptions. This implied that during the film growth some Cl-groups from $TiCl_4$ may have not reacted, which is likely due to steric hindrance of precursor molecules. Moreover, the peak intensities were found to depend in an expected manner on the *k*:*m* ratio, as a further proof of a well-controlled synthesis.

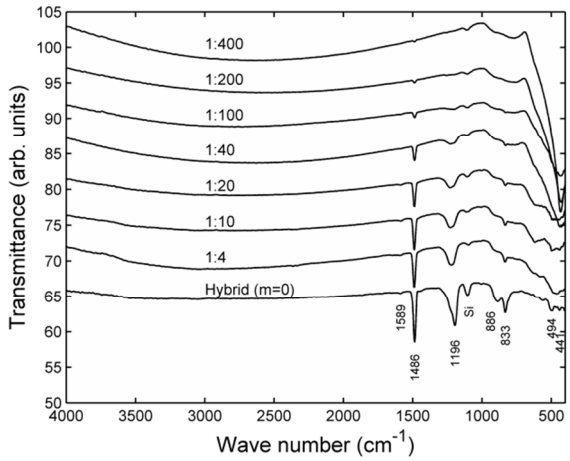

Figure 6. Fourier transform infrared spectra for the $[(TiO_2)_m(Ti\text{-}O\text{-}C_6H_4\text{-}O\text{-})_{k=1}]_n$ thin films for *k*:*m* in the range of 1:400-1:4 and for (*m*=0) hybrid.

Electron and mass densities were estimated for the present films from the XRR patterns. The critical angle θ_c of the reflection curve essentially depends on the mean electron density in the

material $\rho_e = (\theta_c^2\pi)/(\lambda^2 r_e)$, where λ is the x-ray wavelength and r_e the classical electron radius.[28] If one assumes elemental composition for the material can mean mass density then be estimated from $\rho_m = (\rho_e A)/(N_A Z)$, where A is average molar mass, N_A the Avogadro constant and Z the average atomic number.[28] As seen in Fig. 7(a) the critical angle of the reflectivity curves showed a clear reducing trend with increasing *k:m* ratio. This is explained by reduction in overall electron density as is reasonable for increasing organic content (Fig. 7(b)). The estimated mass density values obtained assuming stoichiometry of $[(TiO_2)_m(Ti\text{-}O\text{-}C_6H_4\text{-}O\text{-})_k]$ reduced in line with electron density for increasing fraction of organic content and the control over the *k:m* ratio enabled precise control over the material's density from 3.6 g/cm^3 for pure TiO_2 to 1.6 g/cm^3 for the *m*=0 hybrid (Fig. 7(c)). The value 3.6 g/cm^3 obtained for the present pure TiO_2 thin film approaches the density of bulk anatase[29] 3.84 g/cm^3. This is in line with the previously reported values 3.39–3.76 g/cm^3 for ALD-fabricated TiO_2 films[30] and is in agreement with our XRD data that confirmed growth of anatase phase TiO_2. The value 1.6 g/cm^3 for the *m*=0 hybrid indicates a dramatic decrease in density compared to the purely inorganic films and compares well with the values of around 1.5–2.0 g/cm^3 reported previously for similar types of hybrid films[14,20,21,27]. Such changes in the density values for the present films indicate modification of mechanical properties typically searched for hybrid inorganic-organic films, *e.g.*, for flexible applications.

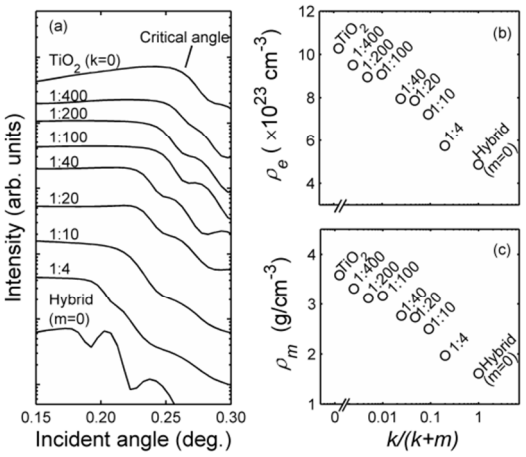

Figure 7. X-ray reflectivity patterns for the $[(TiO_2)_m(Ti\text{-}O\text{-}C_6H_4\text{-}O\text{-})_{k=1}]_n$ films around the critical angle (a). Mean electron densities ρ_e as determined from the critical angles (b) and mass densities ρ_m obtained further assuming elemental composition of $(TiO_2)_m(Ti\text{-}O\text{-}C_6H_4\text{-}O\text{-})$ for the films (c).

The optical characteristics of the films were studied by means of spectrophotometry in the UV-vis range of light at normal angle of incidence. In Figs. 8(a) and 8(b) results are shown for film transmittance T and absorbance A = 1 – (R + T), where R is reflectance, as a function of the photon wave length. Two evident absorption features were seen in the measured wave length range: a sharp increase in absorbance at around 390 nm and a broad maximum at around 400 nm. The first feature around 390 nm was ascribed to fundamental absorption related to electron excitation over the TiO_2 band gap (Figs. 8(c) and 8(d)). The band gaps of the $[(TiO_2)_m(Ti\text{-}O\text{-}C_6H_4\text{-}O\text{-})]_n$ samples were estimated from $(\alpha h\nu)^{1/2}$ vs. $h\nu$ plots for indirect-gap and amorphous semiconductors, where α is the absorption coefficient and $h\nu$ is the photon energy, by extrapolating the linear region of strong absorption to the energy axis (Fig. 8(c)). The absorption coefficient was estimated from the transmittance and reflectance data. The obtained band gap estimate for the pure TiO_2 film of 3.25 eV is in accord with the literature value of 3.2 eV for anatase TiO_2.[31] The TiO_2 band gap was found to blue-shift in the superlattice films with decreasing superlattice period with an onset between periods of 1:20 (0.96 nm) and 1:40 (1.9 nm)

finally reaching 3.75 eV for the m=0 hybrid. The blue-shift is probably due to quantum confinement of electrons with decreasing TiO_2 domain size in analogy to nanocrystalline materials in which a decrease in grain size leads to an increase in the band gap.[32] The present threshold TiO_2 domain size (< 2 nm) for onset for confinement effects is in line with the reported threshold for TiO_2 nanoparticles (< 3 nm).[33] The 0.5 eV increase in the band gap between the pure TiO_2 and hybrid films is in line with the results of Abdulagatov *et al*.[28] and Yoon *et al*.[34]

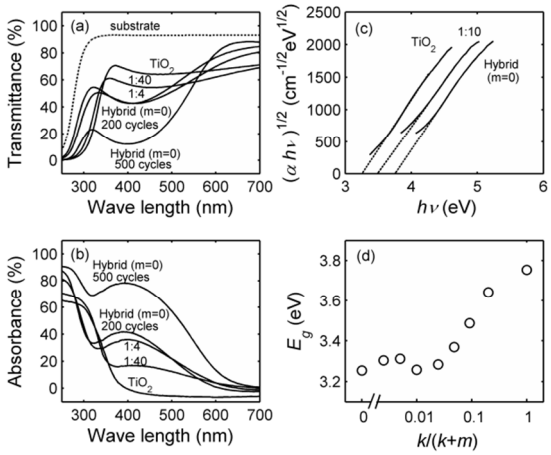

Figure 8. UV-vis (a) transmittance and (b) absorbance for selected $[(TiO_2)_m(Ti\text{-}O\text{-}C_6H_4\text{-}O\text{-})_{k=1}]_n$ films. (c) Illustrative $(\alpha hv)^{1/2}$ vs. hv plots, where α is the absorption coefficient and hv the photon energy, and (d) energy gap values E_g.

The second feature with the 400 nm maximum red-shifted the absorption edge of the samples close to 700 nm extending over a considerable part of the visible range in agreement with orange/red color of the samples. The feature was absent for the pure TiO_2 film and increased in magnitude for increasing (Ti-O-C_6H_4-O-) content in the $[(TiO_2)_m(Ti\text{-}O\text{-}C_6H_4\text{-}O\text{-})_k]_n$ hybrid films. The absorbance of pure hydroquinone peaks slightly below 300 nm,[35] and hence can not explain the broad feature. The fact that the intensity of the feature appeared to depend rather on the amount $k\times n$ of the (Ti-O-C_6H_4-O-) layers than on the superlattice period indicated that the

absorption was not inherent to the superlattice structure; instead it appeared to stem from the local (Ti-O-C_6H_4-O-) environment. Absorption features similar to the present have been observed for TiO_2 nanotube surfaces modified with hydroquinone[35] and for TiO_2 nanoparticle surfaces modified with several enediol ligands.[36] In both the material systems binding over inorganic-organic interface was essentially characterized by Ti-O-C linkages as is for the present samples. It was shown through electron paramagnetic studies that enediol ligands form charge transfer complexes with TiO_2 nanoparticles[36] and supported via computational studies in the case of catechol modifiers that excitation takes place from a molecular orbital of the aromatic ring to an orbital delocalized on a titanium atom in TiO_2 lattice.[37] Taken the similarity between the inorganic-organic interface structures between the present $[(TiO_2)_m(Ti\text{-}O\text{-}C_6H_4\text{-}O\text{-})_k]_n$ thin films and the hybrid systems of Refs. 35-37 it is probable that the observed red-shift for our hybrid thin films is due to excitations from molecular orbitals of the aromatic rings to orbitals delocalized on titanium atoms in TiO_2. Such visible range absorption appears to be unique to the present films among the ALD/MLD hybrids, and particularly, it is in notable contrast to high visible range transmittance reported for films from Diethylzinc and HQ[35] or from $TiCl_4$ and EG/GL[28] precursors. As ALD/MLD particularly excels in conformal depositions on 3D large surface area nanostructured electrodes, the ability to create functional inorganic-organic interfaces with light absorbing organic units together with charge transfer to the TiO_2 body, by a route such as the present, could be promising for solar cell applications. Moreover, hybrid films with TiO_2 surface termination and absorption properties as reported here might show improved photocalytic properties with activity extended to the visible range of light.

Experimental

Fabrication of the thin films was carried out in a Picosun R-100 ALD reactor using N_2 as a carrier

gas for the precursors and as a purging gas. Borosilicate glass and silicon were used as substrates and the deposition temperature was set at 210 ^{o}C for all the depositions. To reach the precursor vapor pressures required for efficient precursor transport to the substrate, HQ was heated up to 120 ^{o}C, whereas $TiCl_4$ and H_2O could be kept at room temperature. Hybrid $(Ti\text{-}O\text{-}C_6H_4\text{-}O\text{-})_k$ thin films were grown from $TiCl_4$ and HQ precursors with varying the total number of deposition cycles, *k* (Fig. 1(a)). After optimizing the process for self-saturating surface reactions, each $TiCl_4$/HQ cycle to deposit a monolayer of the hybrid film was fixed to the following pulsing sequence: $TiCl_4(0.2s)/N_2(4s)/HQ(15s)/N_2(30s)$. Hybrid $[(TiO_2)_m(Ti\text{-}O\text{-}C_6H_4\text{-}O\text{-})_{k=1}]_n$ superlattice structures were then fabricated by mixing the deposition process for hybrid $(Ti\text{-}O\text{-}C_6H_4\text{-}O\text{-})_k$ films with the $TiCl_4/H_2O$ ALD process for TiO_2 (Fig. 1(b)). To deposit one ALD cycle of TiO_2, the precursors were pulsed in the following manner: $TiCl_4(0.2s)/N_2(4s)/H_2O(0.1s)/N_2(4s)$.[27] In the mixed process, at first a TiO_2 layer was deposited via *m* $TiCl_4/H_2O$ cycles, then a single cycle (*k=1*) of $(Ti\text{-}O\text{-}C_6H_4\text{-}O\text{-})_{k=1}$ hybrid was grown on top of the TiO_2 layer. These two steps were then repeated *n* times in order to fabricate thin films with superlattice structures. Hence, the *k:m* ratio was effectively used to control the superlattice period and *n* was the number of superlattice period repetitions. In terms of *m*, *k* and *n*, the total number of deposition cycles was obtained as $(m+k)\times n$. A wide range of compositions was studied varying the *k:m* ratio between 1:400 and 1:4.

The structure of the grown thin films was studied with X-ray scattering techniques using a PANanalytical X'Pert Pro MPD diffractometer, with Cu K_α radiation, as the instrument. For determination of the film crystallinity the diffractometer was operated at low angle of incidence, *i.e.*, grazing incidence X-ray diffraction (GIXRD) geometry was used. Film thicknesses were determined by means of X-ray reflectivity (XRR) and the growth per cycle values calculated dividing the measured thicknesses by the total number of deposition cycles. In particular, the

XRR technique was used to observe the characteristic reflection patterns for the superlattice films. Furthermore, estimates for film densities were calculated from the critical angles θ_c of the XRR curves.

The chemical state of the films was determined employing a Fourier transform infrared (FTIR) Nicolet magma 750 spectrometer. The samples deposited on silicon substrates were used for the IR measurements and were scanned for their IR response in the wave number range of 400-4000 cm^{-1} in transmission mode. The spectrum of a bare substrate was subtracted from the sample data to obtain the actual spectra for the thin films.

The samples were characterized for their normal transmittance and reflectance in the UV-Vis wave length range 200-1100 nm with Hitachi U-2000 spectrophotometer. The measured reflectance spectra were referenced against a spectrum for an aluminum mirror. Absorbance of the films was deduced from the transmittance and reflectance data and the band gaps were estimated from the plots of square root of absorption coefficient vs. photon energy.

Conclusions

In this work we deposited hybrid inorganic-organic $(Ti\text{-}O\text{-}C_6H_4\text{-}O\text{-})_k$ thin films from $TiCl_4$ and HQ precursors with a combined ALD/MLD technique. The film growth proceeded via self-saturated surface reactions in a linear fashion with respect to the number of deposition cycles yielding an average film growth of 3.1 Å/cycle at 210 ^oC. Thin films having $[(TiO_2)_m(Ti\text{-}O\text{-}C_6H_4\text{-}O\text{-})_{k=1}]_n$ superlattice structures with a composition in the range of $1{:}4 \leq k{:}m \leq 1{:}400$ were fabricated by mixing the process developed for hybrid $(Ti\text{-}O\text{-}C_6H_4\text{-}O\text{-})_k$ films with the ALD process for TiO_2 from $TiCl_4$ and H_2O. A proof of successful fabrication of the targeted superlattice structures

was seen in the characteristic XRR patterns that stemmed from periodically arranged well-defined inorganic-organic interfaces. It was determined from the FTIR spectra that the benzene rings from the HQ precursor molecules were delivered to the superlattice structure intact and that they bonded via oxygen atoms to the TiO_2 layers. The deposition of the organic layers between the TiO_2 layers was found to inhibit film crystallization in a way that the 1:400 sample showed weakly crystalline character and otherwise our ALD/MLD process yielded amorphous superlattice films. The density of the films was systematically reduced with increasing organic content from 3.6 g/cm^3 for pure TiO_2 to 1.6 g/cm^3 for the *m*=0 hybrid, indicating improved mechanical properties highly interesting for flexible applications. Probable indication of quantum confinement of electrons in the TiO_2 layers was seen as the optical band gap of the superlattices blue-shifted with decreasing superlattice period up to 3.75 eV for *m*=0 hybrid from 3.25 eV for purely inorganic TiO_2 film. The addition of the organic layers sensitized the TiO_2 layers to visible light in a way that absorption started from around 700 nm. Such a sensitization of TiO_2 to visible light by the present method appears interesting for photocatalysis and solar cell applications particularly when conformal coating of nanostructured electrodes is required.

Acknowledgements

The present work has received funding from the European Research Council under the European Union's Seventh Framework Programme (FP/2007-2013)/ERC Advanced Grant Agreement (No. 339478), the Academy of Finland (No. 255562), and the Aalto Energy Efficiency Research Programme.

Notes and references

1 C. Sanchez, C. Boissiere, S. Cassaignon, S. Chaneac, O. Durupthy, M. Faustini, D. Grosso, C. Laberty-Robert, L. Nicole, D. Portehault, F. Ribot, L. Rozes, C. Sassoye, *Chem. Mater.*, 2014, **26**, 221-238.

2 C. Sanchez, B. Lebeau, F. Chaput, J.-P. Boilot, *Adv. Mater.*, 2003, **15**, 1969-1994.

3 D. B. Mitzi, K. Chondroudis, C. R. Kagan, *IBM J. Res. & Dev.*, 2001, **45**, 29-45.

4 L. Wang, M.-H. Yoon, G. Lu, Y. Yang, A. Facchetti, T. J. Marks, *Nature Mater.*, 2006, **5**, 893-317.

5 X. Huang, J. Li, *J. Am. Chem. Soc.*, 2007, **129**, 3157-3162.

6 T. Suntola, *Mater. Sci. Rep.*, 1989, **4**, 261-312.

7 M. Leskelä, M. Ritala, *Thin Solid Films*, 2002, **409**, 138-146.

8 S. M. George, *Chem. Rev.*, 2010, **110**, 111-131.

9 V. Miikkulainen, M. Leskelä, M. Ritala, R. L. Puurunen, *J. Appl. Phys.*, 2013, **113**, 021301-(1-100).

10 S. M. George, B. Yoon, A. A. Dameron, *Acc. Chem. Res.*, 2009, **42**, 498-508.

11 B. H. Lee, B. Y. Yoon, A. I. Abdulagatov, R. A. Hall, S. M. George, *Adv. Funct. Mater.*, 2013, **23**, 532-546.

12 Y. Du, S. M. George, *J. Phys. Chem. C*, 2007, **111**, 8509-8517.

13 M. Putkonen, J. Harjuoja, T. Sajavaara, L. Niinistö, *J. Mater. Chem.*, 2007, **17**, 664-669.

14 A. A. Dameron, D. Seghete, B. B. Burton, S. D. Davidson, A. S. Cavanagh, J. A. Bertrand, S. M. George, *Chem. Mater.*, 2008, **20**, 3315-3326.

15 P. Sundberg, M. Karppinen, *Beilstein J. Nanotechnol.* 2014, **5**, 1104-1136.

16 Q. Peng, B. Gong, R. M. VanGundy, G. N. Parsons, *Chem. Mater.*, 2009, **21**, 820-830.

17 K. P. Klepper, O. Nilsen, H. Fjellvåg, *Dalton Trans.*, 2010, **39**, 11628-11635.

18 K. P. Klepper, O. Nilsen, P.-A. Hansen, H. Fjellvåg, *Dalton Trans.*, 2011, **40**, 4636-4646.

19 B. H. Lee, B. Yoon, V. R. Anderson, S. M. George, *J. Phys. Chem. C*, 2012, **116**, 3250-3257.

20 P. Sundberg, A. Sood, X. Liu, L.-S. Johansson, M. Karppinen, *Dalton Trans.*, 2012, **41**, 10731-10739.

21 P. Sundberg, A. Sood, X. Liu, L.-S. Johansson, M. Karppinen, *Dalton Trans.*, 2013, **42**, 15043-15052.

22 K.-H. Yoon, K.-S. Han, M.-M. Sun, *Nanoscale Res. Lett.*, 2012, **7**, 71-(1-6).

23 T. Tynell, I. Terasaki, H. Yamauchi, M. Karppinen, *J. Mater. Chem. A*, 2013, **1**, 13619-13624.

24 T. Tynell, H. Yamauchi, M. Karppinen, *J. Vac. Sci. Technol. A*, 2014, **32**(1), 01A105-(1-5).

25 A. Fujishima, K. Honda, *Nature*, 1972, **238**, 37-38.

26 B. O'Regan, M. Grätzel, *Nature*, 1991, **353**, 737-740.

27 A. I. Abdulagatov, R. A. Hall, J. L. Sutherland, B. H. Lee, A. S. Cavanagh, S. M. George, *Chem. Mater.*, 2012, **24**, 2854-2863.

28 V. Holy, U. Pietsch, T. Baumbach, *High Resolution X-Ray Scattering from Thin Films and Multilayers*, Springer-Verlag: Berlin, 1999, p. 127.

29 *CRC Handbook of Chemistry and Physics*, 70th edn., CRC Press: Boca Raton, 1989, p. B-140.

30 M. Ritala, M. Leskelä, E. Nykänen, P. Soininen, L. Niinistö, *Thin Solid Films*, 1993, **225**, 288-295.

31 H. Tang, K. Prasad, R. Sanjinès, P. E. Schmid, F. Lévy, *J. Appl. Phys.*, 1994, **75**, 2042-2047.

32 L. Brus, *J. Phys. Chem.*, 1986, **90**, 2555-2560.

33 C. Kormann, D. W. Bahnemann, M. R. Hoffmann, *J. Phys. Chem.*, 1988, **92**, 5196-5201.

34 B. Yoon, B. H. Lee, S. M. George, *J. Phys. Chem. C*, 2012, **116**, 24784-24791.

35 Y. Jia, A. Kleinhammes, H. Kulkarni, K. McGuire, L. E. McNeil, Y. J. Wu, *Nanosci. Nanotechnol.*, 2007, **7**, 458-462.

36 T. Rajh, L. X. Chen, K. Lucas, T. Liu, M. C. Thurnauer, D. M. Tiede, *J. Phys. Chem. B*, 2002, **106**, 10543-10552.

37 P. C. Redfern, P. Zapol, L. A. Curtis, T. Rajh, M. C. Thurnauer, *J. Phys. Chem. B*, 2003, **107**, 11419-11427.

38 J.-P. Niemelä, H. Yamauchi, M. Karppinen, *Thin Solid Films*, 2014, **551**, 19-22.

A combined atomic/molecular layer deposition (ALD/MLD) process can be used to fabricate inorganic-organic $[(TiO_2)_m(Ti\text{-}O\text{-}C_6H_4\text{-}O\text{-})]_n$ superlattice structures where single organic layers are periodically sandwiched between thicker (m>1) TiO_2 layers. The incorporation of organic layers provides us with a means to systematically control the optical properties of TiO_2 thin films, a fact that could be of substantial interest in photocatalysis and solar cell applications.